Earthquake Forecasting Models and their Impact on the Ground Motion Hazard in the Marmara Region, Turkey

A. Akinci[(1)], M. Murru[(1)], R. Console[(2)], G. Falcone[(1)], S. Pucci[(1)]

(1) Istituto Nazionale di Geofisica e Vulcanologia, Rome, Italy
(2) Center of Integrated Geomorphology for the Mediterranean Area, Potenza, Italy

1. Introduction

We calculate the probability of occurrence of earthquakes $M_w > 6.5$ for individual fault sources in the Marmara region for 5, 10, 30 and 50-year periods (starting from January 1th, 2013) using time-independent and time-dependent earthquake forecasting models. The use of geologic data incorporates the long-term recurrence behavior of active faults and the earthquake recurrence rates of individual fault sources derived from slip rate and magnitude using the characteristic earthquake model (Wesnousky, 1994). In order to express the time dependence of the seismic processes to predict the future ground motions that will occur across the region, we used a Brownian Passage Time (BPT) model (Matthews et al., 2002) that is characterized by a mean recurrence time, uncertainty in the recurrence distribution, and elapsed time since the last earthquake. We also used a methodology based on the fusion of the BPT renewal model with a physical model that considers the earthquake probability perturbation for interacting faults by static Coulomb stress changes (King et al., 1994). We treat the uncertainties in the slip rate, characteristic magnitude and aperiodicity of the statistical distribution associated to each examined fault source, by a Monte Carlo technique. The Monte Carlo samples for all these parameters are drawn from a uniform distribution within their uncertainty limits.

In order to evaluate the sensitivities of the earthquake probability models to ground motion hazard we attempt to calculate the probabilistic seismic hazard in the study region. The probabilistic seismic hazard maps of Marmara region are generated by the same procedure used for seismic hazard assessment in United States (Petersen et al., 2008). We adopted empirical Ground Motion Prediction Equations, GMPEs, for assessing the ground shaking hazard as defined by Akkar and Bommer (2010).

We observed that the impact of the different occurrence models on the seismic hazard estimate is quite high; the hazard may further increase up to 50% or more or may decrease by as much as 50% depending on the selected occurrence model in the selected sites. This difference mostly depends on the time elapsed after the latest major earthquake on a specific fault.

In this study, we give the probabilities of occurrence for the next characteristic earthquake, considering the 10^{th}, 50^{th} and 90^{th} percentiles of the Monte Carlo distribution, over the future 50 years, starting on 1 January 2013, considering the information on used parameter uncertainties in the Marmara region. We then attempt to calculate the fault-based probabilistic seismic hazard maps (PSHA) of mean Peak Ground Acceleration (PGA) having 10% probability of exceedence in 50 years on rock site condition from those three forecasting models. Finally, we demonstrate the earthquake occurrence model uncertainty, and the sensitivity of the ground motion hazard for different earthquake recurrence models reporting those of the percentage ratio between the Poisson, BPT and BPT+ΔCFF models.

2. Tectonic Setting

The Marmara region is located at the western end of the North Anatolian Fault Zone (NAFZ). NAFZ splays into three strands in the Marmara region (Barka 1991). The lack of macro-seismicity is located between the 28°-29° longitudes which correspond to the northern border of the Marmara Sea (Ambraseys, 1970; Stein et al., 1997). This gap has a length of 150 km and is therefore capable of generating an earthquake with magnitude similar to that of the Izmit earthquake (Hubert-Ferrari et al., 2000; Parsons et al., 2000). The return period for large earthquakes south of Istanbul varies between 100-1000 years depending on the magnitude of earthquakes and the considered slip rates (GPS=15 mm/y. geological=2-4 mm/y). The latest major large earthquake on this segment was probably in 1509 AD, (intensity, IX). Stein et al. (1997) showed the earthquake-induced Coulomb stress changes on adjacent fault segments. Application of this technique to evaluate the effect of the recent Kocaeli earthquake (1999, M_w=7.4) on neighboring faults, shows an area of increased stress to the east, including the Düzce fault which ruptured just after the Kocaeli earthquake (12 November, 1999, M_w=7.2). To the west, both the 80 km-long Yalova segment, southeast of Istanbul, and the Northern Boundary fault, immediately south of Istanbul, may be close to failure (Hubert-Ferrari et al., 2000). In spite of active morphological expressions along the middle strands from the Mudurnu valley (from the 1967, M_w=7.2, earthquake) to the Aegean Sea, there are only a few possible earthquakes for the last 1000 years which can be associated with this strands. Thus, almost the entire middle strands can be considered as a potential site for large earthquakes. Together with that during the last two centuries, the greatest part of the southern strands has been ruptured as a result of large earthquakes. However, two possible seismic gaps still exist; the Pazarkoy-Edremit gap (60 km long with a double bend geometry separated from the 1953, M_w=7.1 rupture segment by about 12 km wide restraining stopover), and the Yenisehir gap (has a pull-apart geometry). This branch also shows a larger cluster of seismicity near the fourth biggest city of Turkey, Bursa. The area demonstrates several typical aspects of the regional seismotectonic activity and has been subjected to several large earthquakes in the last centuries (28/02/1855, M_w=7.4 and 11/04/1855, M_w=6.8).

Besides very high earthquake hazard, the earthquake risk in those cities has been increasing steadily due to overcrowding, improper land-use planning and construction, inadequate infrastructure and services, and environmental degradation. Because of the real earthquake threat in the Marmara region, the need for seismic hazard studies has become progressively more important for earthquake engineering applications. Recently, seismic hazard in Istanbul has been estimated using probabilistic methods (Atakan et al., 2002; Erdik et al., 2004).

3. Probability of Occurrence for the Fault Segmentation in the Marmara Region

We calculated the probability of occurrence for the fault segmentation in the Marmara region using the Poisson model for time intervals of 5-10-30 and 50 years starting from January 1, 2013. These probabilities are shown in Tab. 1. We note that the maximum values of the Poisson probability are on those faults that have a high long-term slip rate value. This value has an influence on the mean recurrence time and consequently high values of slip rate reduce the inter-event time. In fact if we examine the latest two events occurred in the Marmara region on the Izmit (August 17, 1999, M_w7.4) and Duzce (November 12, 1999, M_w7.1) faults, we will note on these fault sources two of the highest Poisson values. For both faults the value of long-term slip rate is equal to 15±3 mm per year.

The BTP probability is larger than the Poisson probability in the case when the characteristic event has occurred long time ago and the elapsed time is closer to the inter event time. If we consider the 50th percentile for the next 50 years, the largest values will be for West Marmara and Cinarcik faults, in the northern part of Marmara Sea, near the city of Istanbul. For Iznik fault, whose latest event is reported in 121 AD, if we consider the 50th percentile we will obtain for the next 50 years, a BPT probability equal to 8.01% with respect to a 3.78% Poisson probability. The larger value for the BPT time-dependent model is explained by the very long time elapsed after the latest characteristic event on this fault. The BPT probabilities for the Izmit and Duzce faults are lower than the Poisson values due to the short elapsed time (14 years) after the occurrence of their last characteristic events.

The time–dependent hazard rate obtained by the BPT distribution on each fault is successively modified by the inclusion of a permanent physical effect due to the Coulomb static stress change caused by failure of neighboring faults since the latest characteristic earthquake on the fault of interest. We treat again in this step the uncertainties in the recurrence time, co-seismic slip, and magnitude, by a Monte Carlo technique, related to each fault. The Monte Carlo samples for all these parameters are drawn from a uniform distribution within their uncertainty limits. The probability values for Cinarcik, and South Cinarcik show a small difference (±1%) between the two models. This variation is due to a positive (Cinarcik) or negative (South Cinarcik) fault interaction. The largest difference between the two models is visible on the North Saroz fault. In this last case, the BPT probability is larger (22.6%) than the BPT probability with interaction (16.5%).

4. Implications on the Probabilistic Seismic Hazard Maps

We also demonstrate the earthquake occurrence model uncertainty, and the sensitivity of the ground motion hazard for different earthquake recurrence models. Fig. 1a, b and c reports the percentage ratio between the seismic hazard computed with the three earthquake occurrence models (Poisson, BPT and BPT+ΔCFF models, respectively). It is presented as a relative difference in percentage, computed as:

$$[PSHA_{model1} – PSHA_{model2}] / PSHA_{model2} * 100.$$

In generally, the PSHA results based on the time-independent and time-dependent earthquake occurrence models display the effect of the fault recurrence rate and the regency of fault rupture by drastically reducing hazard levels along the eastern part of the North Anatolian Fault Zone by up to 50% nearby Izmit (1), Duzce (11), Gonen (22), Biga (23) and Pazarkoy (24) areas. The strongest effect may be caused by the recurrence rates and the lapse time ratio of the faults and rarely by the maximum magnitude since the models associate same magnitudes to each fault. The areas affected by the recurrence rate change get larger and/or bigger in the time-dependent earthquake occurrence model than the time-independent one. The faults where the BPT probabilities are smaller than the Poisson ones can easily be seen in Fig. 1a, b and c; areas with blue color indicate the decrease in the seismic hazard in terms of ground accelerations. The seismic hazard around faults number 1, 10 and 11 decreases strongly from 0.55 to 0.25 g (up to 50% of change) when the earthquake occurrence model changes from the Poisson to the renewal models, respectively. For faults 15, 18 and 21 seismic hazard increases up to 50% when the renewal models are chosen for the hazard calculation.

Between models BPT and BPT+ΔCFF, the effectiveness of the model chosen is lower at the PGA estimation; the increase is up to 20% and the decrease is up to 30%. The areas affected by the model chosen are much smaller but approximately at the same geographic points except for the North Saros Fault (7). At Southern North Anatolian Fault Strands; Pazarkoy (24), Can (25) and Ezine (26) of and the North Saros (7) fault we observed 5% and 10% of increase in the seismic hazard due to the positive fault interaction, respectively.

#	Fault name	M_w	Elapsed Time	Elapsed Time Ratio	Poisson 50 year prob. 50th percent.	BPT 50 year prob. 50th percent.	BPT+ΔCFF 50 year prob. 50th percent.
1	Izmit	7,4±0,2	14	0.12	3.61E-01	5.40E-03	5.79E-03
2	Cinarcik	7,0±0,2	119	0.88	3.29E-01	5.50E-01	5.55E-01
3	S.Cinarcik	6,8±0,2	259	1.04	1.95E-01	3.59E-01	3.45E-01
4	C.Marmara	7,2±0,2	247	1.27	2.23E-01	4.18E-01	4.19E-01
5	W.Mar.	7,2±0,3	457	2.92	2.82E-01	5.32E-01	5.33E-01
6	Ganos	7,4±0,2	101	0.47	2.16E-01	2.66E-01	2.67E-01
7	N. Saros	7,1±0,2	120	0.49	1.88E-01	2.26E-01	1.65E-01
8	S. Saros	7,1±0,2	154	0.62	1.83E-01	2.64E-01	2.79E-01
9	Mudurnu	7,2±0,2	46	0.23	2.32E-01	1.21E-02	1.17E-03
10	Abant	7,2±0,2	56	0.22	1.85E-01	2.13E-03	3.88E-03
11	Duzce	7,1±0,2	14	0.09	2.78E-01	4.11E-02	4.11E-02
12	Gerede	7,5±0,2	69	0.42	2.53E-01	2.61E-01	2.53E-01
13	Geyve	7,0±0,3	717	2.45	1.59E-01	3.32E-01	3.08E-01
14	Iznik	7,4±0,3	1892	1.47	3.78E-02	8.01E-02	7.60E-02
15	Yenisehir	6,8±0,3	948	2.11	1.05E-01	2.19E-01	2.12E-01
16	Gemlik	6,8±0,2	158	0.40	1.53E-01	1.88E-01	1.50E-01
17	Bursa	6,8±0,2	163	0.91	2.51E-01	4.32E-01	4.33E-01
18	S.Marmara	7,1±0,3	457	0.87	1.15E-01	2.19E-01	2.09E-01
19	Kemalpasa	7,4±0,2	158	0.14	2.09E-02	4.72E-10	1.06E-09
20	Manyas	6,9±0,2	49	0.32	3.44E-01	4.04E-01	3.99E-01
21	Bandirma	7,0±0,3	1890	3.24	1.02E-01	2.12E-01	2.12E-01
22	Gonen	7,1±0,2	60	0.12	9.83E-02	9.46E-04	6.25E-04
23	Biga	7,0±0,2	44	0.10	1.21E-01	1.16E-03	1.24E-03
24	Pazarkoy	6,8±0,2	69	0.21	1.77E-01	7.76E-02	6.20E-02
25	Can	7,0±0,2	276	0.61	1.12E-01	1.65E-01	1.32E-01
26	Ezine	7,0±0,2	187	0.29	7.93E-02	2.89E-02	2.80E-02

Tab. 1 Marmara Fault segmentations and the calculated probabilities of occurrence together with the elapsed time ratio on the fault (lapsed-time / recurrence time), for a 50-year period of time (2013–2063) according to the Poisson, BPT and BPT with a stress interaction models for each fault segment of the Marmara region. The probability values related to 50th percentile are shown in the table.

Fig. 1 It represents the ratio between the 50th percentiles PGA seismic hazard for **a)** Poisson and BPT (%10 in 50 years) **b)** Poisson and BPT+ΔCFF (%10 in 50 years), **c)** BPT and BPT+ΔCFF (%10 in 50 years) calculated using the fault segments only. In red: positive amplifications. In blue: negative amplifications. Black lines represent the surface ruptures of each fault numbered as in **Table 1.**

5. Acknowledgements

This work has been partially supported by the MARSite (Marmara Supersite) “New Directions in Seismic Hazard Assessment through Focused Earth Observation in the Marmara Supersite”, European Integrated Project, THEME-ENV.2012.6.4-2 (Long-term monitoring experiment in geologically active regions of Europe prone to natural hazards: the Supersite concept), Grant Agreement No: 308417.

6. References

Akkar S. and Bommer J.J.; 2010: *Empirical equations for the prediction of PGA, PGV, and spectral Accelerations in Europe, the Mediterranean, and the Middle East*.Seismol. Res. Lett., **81 (2)**, 195–206.

Ambraseys N.; 1970: *Some characteristic features of the Anatolian fault zone*, Tectonophysics, **9**, 143-65.

Atakan K, Ojeda A, Meghraoui M, Barka AA, Erdik M, Bodare A.; 2002: *Seismic hazard in Istanbul following the 17 August 1999 Izmit and 12 November 1999 Duzce earthquakes*. Bull Seism Soc Am, **92**, 466–82.

Barka A.A.; 1992: *The North Anatolian Fault Zone*, Ann. Tecton., **6**, 164–195.

Erdik M., Demircioglu M., Sesetyan K., Durukal E., Siyahi B.; 2004: *Earthquake hazard in Marmara Region,Turkey*, Soil Dynamics and Earthquake Engineering, **24**, 605-631.

Hubert-Ferrari A., Armijo R., King G., Meyer B., Barka A. ; 2002: *Morphology, displacement, and slip rates along the North Anatolian Fault, Turkey*, J. Geophys. Res., **107(B10)**, 2235, doi:10.1029/2001JB000393.

King G. C. P., Stein R. S., Lin J.; 1994: *Static stress changes and the triggering of earthquakes*, Bull. Seismol. Soc. Am., **84**, 935–953.

Matthews M. V., Ellsworth W. L., Reasenberg P.A.; 2002: *A Brownian model for recurrent earthquakes*, Bull. Seismol. Soc. Am., **92**, 2233–2250.

Parson T., Toda S., Stein R.S., Barka A., Dietrich J.H.; 2000: *Heightened odds of large earthquakes near Istanbul: an interaction-based probability calculation*, Science, **288**, 661-665.

Petersen M. D., Frankel A. D., Harmsen S. C., Mueller C. S., Haller K. M, Wheeler R. L., Wesson R. L., Zeng Y., Boyd O. S., Perkins D. M., Luco N., Field E. H., Wills C. J., Ruksatles K. S.; 2008:. *Documentation for the 2008 update of the United States national seismic hazard maps*, U.S. Geol. Surv. Open-File Rept., **2008–1128**,60 pp.

Stein R., Barka A., Dieterich J.; 1997*: Progressive failure on the North Anatolian fault since 1939 by earthquake stress triggering*, Geophys. J. Int., **128**, 594-604.

Wesnousky S. G.; 1994:*The Gutenberg-Richter or characteristic earthquake distribution, which is it?*, Bull. Seismol. Soc. Am., **84**, 1940-1959.

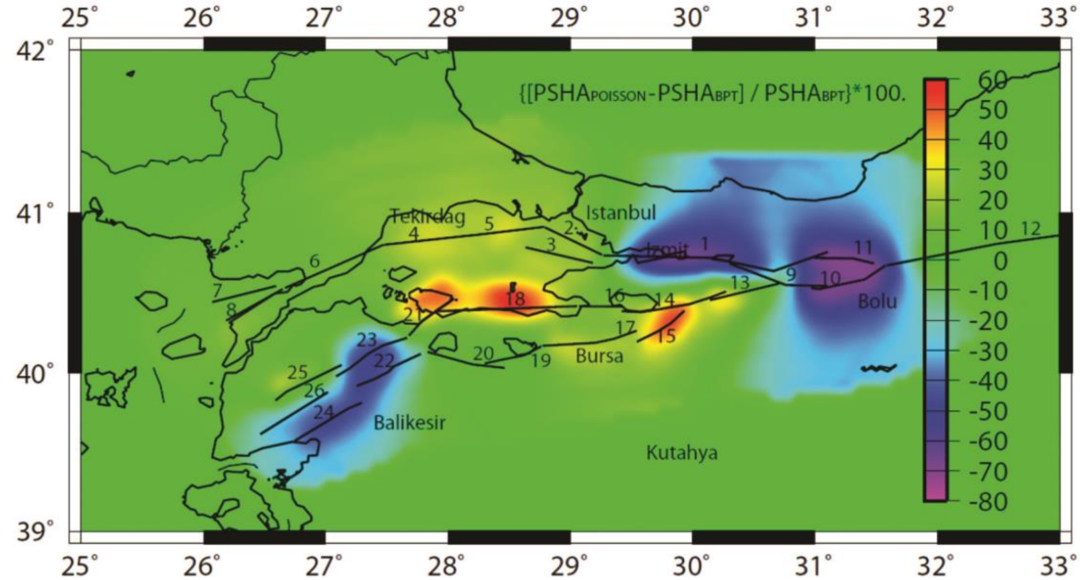
{[PSHAPOISSON-PSHABPT] / PSHABPT}*100.
60 50 40 30 20 10 0 -10 -20 -30 -40 -50 -60 -70 -80
25° 26° 27° 28° 29° 30° 31° 32° 33°
39° 40° 41° 42°
Tekirdag
Istanbul
Izmit
Bolu
Bursa
Balikesir
Kutahya

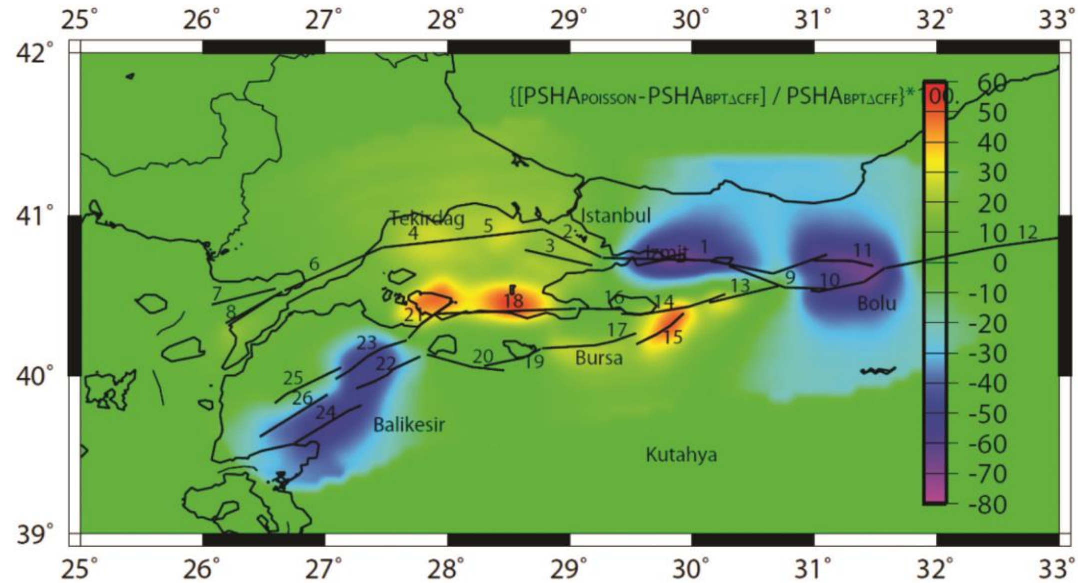
{[PSHAPOISSON-PSHABPTΔCFF] / PSHABPTΔCFF}*100.
60 50 40 30 20 10 0 -10 -20 -30 -40 -50 -60 -70 -80
25° 26° 27° 28° 29° 30° 31° 32° 33°
39° 40° 41° 42°
Tekirdag
Istanbul
Izmit
Bolu
Bursa
Balikesir
Kutahya

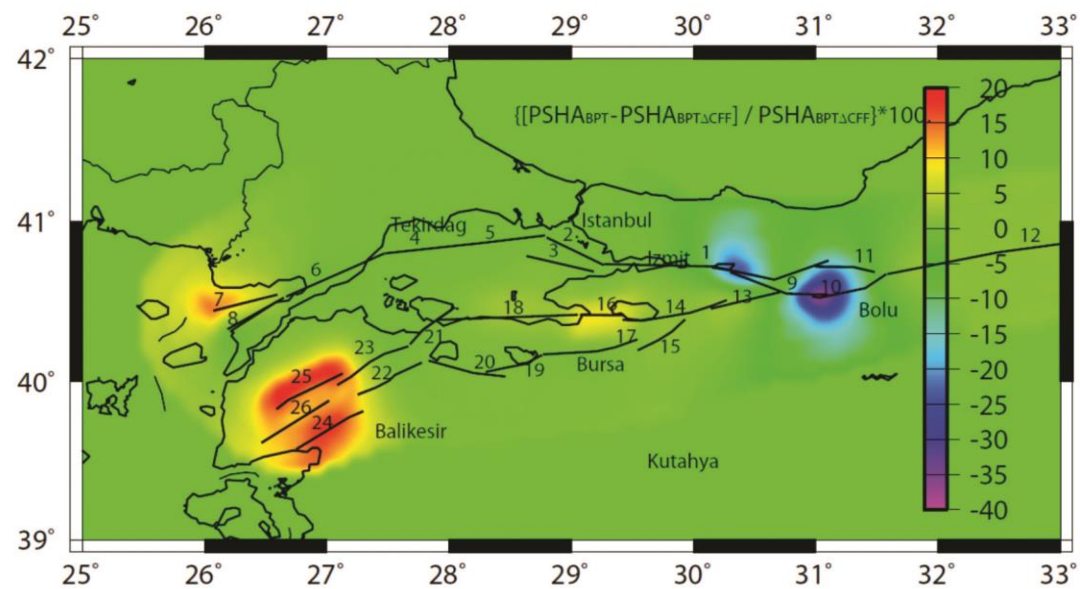
{[PSHABPT-PSHABPTΔCFF] / PSHABPTΔCFF}*100.
20 15 10 5 0 -5 -10 -15 -20 -25 -30 -35 -40
25° 26° 27° 28° 29° 30° 31° 32° 33°
39° 40° 41° 42°
Tekirdag
Istanbul
Izmit
Bolu
Bursa
Balikesir
Kutahya